



Published in final edited form as:

J Nat Prod. 2011 October 28; 74(10): 2313–2317. doi:10.1021/np200610t.

A Cannabinomimetic Lipid from a Marine Cyanobacterium

Marcelino Gutiérrez^{*,†,‡}, Alban R. Pereira[†], Hosana M. Debonis^{†,§}, Alessia Ligresti[⊥], Vincenzo Di Marzo[⊥], and William H. Gerwick^{*,†}

[†]Center for Marine Biotechnology and Biomedicine, Scripps Institution of Oceanography, and Skaggs School of Pharmacy and Pharmaceutical Sciences, University of California, San Diego, La Jolla, California 92093, United States

[‡]Instituto de Investigaciones Científicas y Servicios de Alta Tecnología, Ciudad del Saber, Clayton 0843-01103, Panamá

[§]Departamento de Física e Química, Faculdade de Ciências Farmacêuticas de Ribeirão Preto-Universidade de São Paulo, Ribeirão Preto, São Paulo 14040903, Brazil

[⊥]Institute of Biomolecular Chemistry, National Research Council, 80078 Pozzuoli, Italy

Abstract

NMR-guided fractionation of two independent collections of the marine cyanobacteria *Lyngbya majuscula* obtained from Papua New Guinea and *Oscillatoria* sp. collected in Panama led to the isolation of the new lipids, serinolamide A (**3**) and propenediester (**4**). Their structures were determined by NMR and MS data analysis. Serinolamide A (**3**) exhibited a moderate agonist effect and selectivity for the CB₁ cannabinoid receptor (EC₅₀ 2.3 μM, >10-fold), and represents the newest addition to the known cannabinomimetic natural products of marine origin.

An important discovery in neuropharmacological research has been the discovery of specific cannabinoid receptors (CB₁ and CB₂) in central and peripheral mammalian tissues.^{1–3} Both receptor subtypes have amino acid sequences characteristic of G-protein-coupled receptors (GPCR).^{2,4} CB₁ receptors exhibit a widespread distribution in the brain and are responsible for the psychological and anticonvulsive effects produced by marijuana.^{3,4} CB₂ receptors are most abundant in the immune system and they appear to be involved in the anti-inflammatory and possibly other therapeutic effects of cannabis.^{3–5} Thus, CB₂ represents an attractive pharmacological target for developing cannabinoid-based therapeutic agents in the treatment of several human conditions (e.g., cancer, chemotherapy relief, neuropathic pain, neurotrauma, and appetite regulation).⁶

The characterization of the CB₁ and CB₂ receptors has launched the quest for their corresponding endogenous ligands, which led in 1992 to the isolation of the lipid derivative, anandamide (**1**).^{2,7} This endogenous metabolite binds to both CB₁ and CB₂ receptors and is found in nearly all tissues in a wide range of animals.² Besides **1**, several other endogenous fatty acid-derived compounds have been reported that are capable of binding one or both of the cannabinoid receptors.^{6,8} Among them, 2-arachidonoylglycerol (**2**) is more abundant and efficacious than **1**, but as a monoglyceride, it takes part in several other pathways of lipid metabolism that minimizes its availability for endocannabinoid signaling.^{2,9}

*To whom correspondence should be addressed. Tel: (507)-5170732. Fax: (507)-517070. mgutierrez@indicat.org.pa and Tel: (858)-534-0578. Fax: (858)-534-0529. wgerwick@ucsd.edu.

Supporting Information Available. ¹H NMR, ¹³C NMR, and 2D NMR spectra in CDCl₃ of compounds **3** and **4**. This material is available free of charge via the Internet at <http://pubs.acs.org>.

Marine organisms in general, and cyanobacteria in particular, have been a rich source of unusual alkyl amides that resemble structurally some aspects of anandamide and other endocannabinoids.¹⁰ Our group has previously reported cannabinomimetic activity for the chlorosulfolipid malhamensilipin A,^{10c} as well as the fatty acid-based metabolites grenadadiene^{10d} and semiplenamides A, B and G.^{10e}

As part of an ongoing program aimed at characterizing the bioactive natural products of various marine organisms, we investigated the extracts of two independent collections of marine cyanobacteria that shared similar NMR characteristics. The first extract, prepared from a specimen of *Lyngbya majuscula* collected in Papua New Guinea, was fractionated chromatographically to afford the new cannabinoid-active lipid, serinolamide A (**3**), bearing a strong structural similarity to anandamide (**1**). Extracts from this same collection of *L. majuscula* were reported previously to produce the potent cancer cell cytotoxin, apratoxin D, a cyclodepsipeptide metabolite.¹¹ The second extract, derived from a *Oscillatoria* sp. specimen, showed NMR resonances analogous to those of serinolamide A (**3**), and its ¹H NMR-guided fractionation led to the discovery of the new cyanobacterial lipid, propenediester (**4**). Herein, we report the isolation, structure elucidation, and biological activity of serinolamide A (**3**) and propenediester (**4**), two new anandamide-like lipids isolated from marine cyanobacteria.

The marine cyanobacterium *L. majuscula* was collected by hand using scuba from New Ireland in Papua New Guinea. The sample was extracted with CH₂Cl₂-MeOH (2:1) and 8.8 g of the resulting extract was fractionated by silica gel vacuum-liquid chromatography (VLC) to obtain nine fractions (A–I). Further purification of this material using reversed-phase HPLC yielded 2.9 mg (0.03%) of serinolamide (**3**). HRESITOFMS analysis of **3** showed a pseudomolecular ion [M + H]⁺ at *m/z* 384.3479 and its sodium adduct [M + Na]⁺ at *m/z* 406.3295, corresponding with the molecular formula, C₂₃H₄₅NO₃, and indicating that this compound possesses two degrees of unsaturation. IR spectroscopy showed absorptions at 3351 and 1622 cm⁻¹ suggesting the presence of hydroxy and amide-carbonyl groups. The ¹H NMR spectrum of **3** showed resonances for three methyl groups, two of which were consistent with being directly attached to oxygen and nitrogen atoms, respectively [δ 3.33 (s, H-23) and 3.01 (s, H-19)] (Table 1). The third methyl group at δ 0.88 (t, *J* = 6.5 Hz, H-18) showed a chemical shift and multiplicity typical of a terminal methyl group of a fatty acid chain. Furthermore, resonances for 16 methylenes were observed, some of which were deshielded to shifts corresponding to oxymethylenes [δ 3.78 (m, H-20), 3.66 (dd, *J* = 7.0, 10.0 Hz, H-22a), and 3.56 (dd, *J* = 4.5, 10.0 Hz, H-22b)]. Other methylene groups appeared at high field [δ 2.40 (m, H-2), 2.32 (m, H-3), 1.96 (m, H-6), and 1.28 (m, H-17)], which, in combination with a 20H signal at δ 1.25 for ten methylenes and two methine resonances at δ 5.43 (m, H-4) and 5.47 (m, H-5), defined a mono-unsaturated alkyl chain. The remaining resonance in the spectrum of **3** was a deshielded methine resonance at δ 4.39 (m, H-21), and by HSQC, corresponded to nitrogen-bonded methine.

The ¹³C NMR spectrum of **3** showed resonances for only 19 carbon atoms. However, the carbon at δ 29.7 was of larger intensity, indicating a superposition of several carbon atoms as is typical for chemically equivalent methylenes in a fatty acid chain. With 23 carbon atoms assigned to **3** by HRMS analysis, the ¹³C NMR and gHSQC spectra were interpreted to contain three methyl groups, sixteen methylenes, three methines, and one quaternary carbon (Table 1).

Overall, analysis of the NMR data of compound **3** (Table 1) allowed the construction of two substructures (Figure 1A). In the first, a prominent singlet at δ 1.25 ppm (20 H) and a triplet at δ 0.88 (3H) suggested the presence of a mostly saturated fatty acid moiety. COSY and HMBC correlations allowed the assignment of the spin system formed by H-2, H-3, H-4,

H-5 and H-6 (**I**, Figure 1A), and the *trans*-geometry of the C-4/C-5 double bond was assigned based on the δ_C values of C-3 and C-6, which are typical for allylic methylenes of a *trans* double bond.¹² The group of ten overlapped methylenes observed at δ 1.25 ppm was localized between C-6 and C-17 based on COSY and HMBC correlations, completing the assignment of sub-structure **I** (Figure 1A).

The second sub-structure **II** consisted of a dimethyl serinol unit that was elucidated as follows. The spin system formed by H-20, H-21 and H-22 was assigned by COSY and $^{2,3}J$ HMBC correlations. The chemical shifts of carbons C-21 and C-22 were typical for oxygen-bonded methylenes, while the chemical shift of the carbon C-20 indicated that it is attached to nitrogen. Methyl groups at δ 3.01 (H-19) and δ 3.33 (H-23) were attached to the serinol nitrogen and the oxygen at C-22, respectively, on the basis of diagnostic HMBC correlations, thus completing the assignment of sub-structure **II**. Substructures **I** and **II** were connected by HMBC correlations observed between the N-Me protons with carbons C-1 and C-20 as well as correlations observed between H-20 and carbons C-1, C-21 and C-22 (Figure 1A).

The absolute configuration at C-20 of the serinol unit was established via chiral derivatization of **3** with (*R*)- and (*S*)-2-(anthracen-9-yl)-2-methoxyacetic acid (9-AMA), according to the methodology reported by Riguera and coworkers for determining the absolute configuration of β -chiral primary alcohols.¹³ Examination of $\Delta\delta$ values obtained from the *R*- and *S*-ester derivatives **3a** and **3b** led to an *S*-configuration assigned at C-20. For the natural product **3** the priority rules for the substituents change, and thus, serinolamide (**3**) possesses the *R* configuration at C-20.

In the case of the *Oscillatoria* sp., a black mat of cyanobacterial biomass was collected by hand from Isla Canales de Afuera, Panamá. A similar extraction and fractionation strategy produced nine sub-fractions (A–I), for which fraction A (1.3 mg) and B (22.0 mg) displayed similar intriguing ^1H NMR resonances and LC-MS data as for compound **3**. Thus, fractions A and B were combined and subjected to further silica gel column chromatography to afford metabolite **4** (6.6 mg, 0.1%).

HRESIMS of **4** yielded an $[\text{M} + \text{Na}]^+$ peak at m/z 417.2978, which when combined with the NMR data (Table 2), was consistent with the molecular formula, $\text{C}_{24}\text{H}_{42}\text{O}_4$, possessing four degrees of unsaturation (calcd for $\text{C}_{24}\text{H}_{42}\text{O}_4\text{Na}$, 417.2975). Intense IR absorptions at 1746 and 1136 cm^{-1} suggested the presence of double and single carbon-oxygen bonds of an ester functional group. The ^1H NMR spectrum of **4** (Table 2) displayed resonances assignable to a deshielded vinylic proton at δ 7.23 and its coupling partner at δ 5.08, a complex multiplet for two deshielded methylenes between δ 4.76–4.70, six methylene multiplets at δ 2.43, 2.06, 1.99, 1.81, 1.40, and 1.28, as well as nine isochronous methylenes centered at δ 1.25, a methyl singlet at δ 2.07, and a final methyl triplet at δ 0.88. In agreement with these assignments, the ^{13}C NMR spectrum of **4** showed two sp^2 methine carbons at δ 136.9 and 107.4, a methylene carbon at δ 57.9 (adjacent to oxygen), two methyl resonances at δ 20.9 and 14.1, and a series of twelve methylene carbons ranging from δ 35.8 to 22.4. This spectrum was completed by deshielded quaternary carbonyl-type resonances at δ 170.8 and 170.1, as well as a quaternary sp^2 carbon at δ 148.5 and a sp^2 methylene resonance at δ 109.7. Extensive analysis by 2D-NMR methods, including the HSQC, HMBC and COSY spectra, revealed the planar structure of propenediester (**4**) as described below.

The most prominent resonance in the ^1H NMR spectrum of **4** was an apparent singlet centered at δ 1.25, which accounted for a total of 18 protons assigned as methylenes via the HSQC spectrum, and was indicative of a saturated fatty acid chain. COSY data allowed definition of the termini flanking this alkyl chain. At one end an ethyl group was found as

revealed by a methyl triplet at δ 0.88 (H-18, $J = 7.1$ Hz, δ_C 14.1) and a methylene multiplet at δ 1.28 (H-17, δ_C 22.7). The other end was comprised of a 1,1-disubstituted double bond as indicated by a deshielded sp^2 methylene group at δ 4.73 (H-19, apparent d, $J = 16.6$ Hz, δ_C 109.7) and a sp^2 quaternary carbon at δ 148.5 (C-5). The protons for this unusual branching methylene showed both COSY and HMBC correlations with flanking methylenes at δ 1.99 (H-6, apparent t, $J = 7.6$ Hz, δ_C 35.8) and 2.06 (H-4, apparent t, $J = 7.6$ Hz, δ_C 35.1). The former was separated from the C₉ saturated alkyl chain mentioned above by an additional methylene at δ 1.40 (H-7, m, δ_C 27.7), whereas the latter methylene was found to comprise a new spin system with methylenes at δ 1.81 (H-3, tt, $J = 7.4, 7.6$ Hz, δ_C 22.4) and 2.43 (H-3, t, $J = 7.4$ Hz, δ_C 33.3). HMBC correlations from H-3 and H-2 were used to situate an ester-type carbonyl (δ 170.1, C-1) at the end of this spin system, thus completing the elucidation of the major portion of compound **4** (Fragment **III**, Figure 1B).

A second spin system in **4** contained a polarized vinylic pair at δ 7.23 (H-20, dt, $J = 1.5, 6.5$ Hz, δ_C 136.9) and 5.08 (H-21, dt, $J = 6.5, 7.1$ Hz, δ_C 107.4), followed by a deshielded methylene (adjacent to oxygen) at δ 4.72 (H-22, dd, $J = 1.5, 7.1$ Hz, δ_C 57.9), exhibiting vicinal and allylic coupling with H-21 and H-20, respectively (Fragment **IV**). The configuration of the polarized double bond was determined as *Z* on the basis a $^3J_{H_{20},H_{21}}$ value of 6.5 Hz. A HMBC correlation from H-20 to C-1 enabled substructures **III** and **IV** to be connected. Likewise, a HMBC correlation from H-22 with a carbonyl carbon at δ 170.8 (C-23) was used to join **IV** with **V**, identified as an acetyl group comprised by C-23 and the methyl singlet at δ 2.07 (H-24, δ_C 20.9). This completed the structure elucidation of propenediester (**4**), a compound with a uniquely branched fatty acid chain.

Due to the similarity in structural features of metabolites **3** and **4** to those of known endocannabinoids (e.g., **1** and **2**), these were evaluated for cannabimimetic properties in radioligand binding assays specific for human CB₁ and CB₂ receptors. Compound **3** exhibited moderate affinity for the CB₁ cannabinoid receptor with a K_i value of 1.3 μ M, whereas **4** was completely inactive (Table 3). More importantly, **3** appears to be selective for CB₁ (>10-fold). Although other CB₁ agonists (e.g., HU-210, ACEA) exhibit much higher affinity and selectivity over CB₂ receptors, only a handful of marine natural products are reported to show such potency and selectivity for CB₁ receptors.¹⁴ Furthermore, chemical entities exhibiting K_i values in the micromolar range such as **3** potentially can exert cannabimimetic effects in vivo, making them attractive from a therapeutic development perspective. Metabolite **3** was cytotoxic when evaluated in vitro against H-460 human lung cell lines (50 μ g/mL, 0% cell survival; 5 μ g/mL, 60% cell survival), whereas compound **4** was inactive at all tested concentrations (up to 20 μ g/mL). These effects might be ascribed to the potential CB₁ agonist activity of **3**, since CB₁ agonists have been shown to exert cytotoxic effects via either induction of apoptosis or inhibition of proliferation.¹⁵ The lack of cannabinoid-type activity for propenediester (**4**) in these binding assays suggests that moieties containing a hydrogen bond donor at the hydrophilic end of their molecule are required to elicit cannabinoid activity. *N*-Arachidonoyl-L-serine, an endogenous mediator found in mammalian tissues and sharing perhaps a greater chemical similarity with **3** than **1**,¹⁶ was found to be completely inactive in both human CB₁ and CB₂ binding assays (K_i >10 μ M), despite containing a secondary amide group in its chemical structure, and possibly because of the presence of a terminal carboxyl group instead of the methoxy group of **3**.

Biogenetically, the C-1 to C-18 substructure of compounds **3** and **4** is probably derived from a PKS pathway, responsible for the production of fatty acids. The serinol unit in **3** likely originates from serine, which has been reported to be biosynthesized by cyanobacteria from phosphoglycerate through the phosphorylated pathway.¹⁷ Incorporation of *N*-Me and *O*-Me groups in the serinol residue of compound **3** occurs presumably via SAM-dependent methyltransferases.¹⁸ In the case of compound **4**, its intriguing 1,1-disubstituted double bond

branch at C-5 resides at a predicted carbonyl site in the nascent polyketide, and thus, is probably produced by a β -branch mechanism involving an HMG-CoA synthase cassette¹⁹ followed by dehydration to generate the double bond. Although highly speculative, it is tempting to attribute fragment **IV** in **4** to glycerol, which would undergo elimination of its middle substituent (C-21 in **2**) through a more stable secondary intermediate (elimination at C-20 or C-22 would involve a primary intermediate).

Experimental Section

General Experimental Procedures

Optical rotations were measured on a JASCO P-2000 polarimeter, whereas UV data was obtained using a Beckman DU800 spectrophotometer. IR spectra were recorded on a Nicolet 100 FT-IR spectrometer. ¹H, ¹³C, and 2D NMR spectra were collected at a ¹H resonance frequency of either 600 MHz (Bruker Avance III DRX600 equipped with a 1.7 mm TCI cryoprobe) or 500 MHz (Varian INOVA 500). Chemical shifts were calibrated internally to the residual signal of the solvent in which the sample was dissolved (CDCl₃, δ_{H} 7.26, δ_{C} 77.0; DMSO-*d*₆, δ_{H} 2.50, δ_{C} 39.5). High-resolution mass spectra were obtained on a ThermoFinnigan MAT900XL mass spectrometer. HPLC was carried out using a dual Waters 515 pump system equipped with a Waters 996 photodiode array detector. Vacuum and flash chromatographic separations were performed using silica gel type H (10–40 μm , Aldrich) and silica gel 60 (40–63 μm , EMD), respectively. Merck TLC sheets (silica gel 60 F254) were used for analytical TLC (aluminum-supported, layer-thickness 200 μm) and preparative TLC (glass-supported, layer-thickness 250 μm). All solvents were purchased as HPLC grade. Cytotoxicity to H-460 cells was determined as previously reported.²¹

Cyanobacterial Collections and Taxonomic Identification

The marine cyanobacterium *Lyngbya majuscula* (voucher specimen available from W.H.G. as collection code: PNG 5-22-05-3) was collected by scuba at a depth of 15 m from New Ireland, Papua New Guinea in May 2005 (S 3°49.626', E 152°26.017'). Specimens of *Oscillatoria* sp. (voucher specimen available from W.H.G. as collection code: PAC-17-FEB-10-3) were collected by hand at a depth of 1–1.5 m on flat rocks at Isla Canales de Afuera, Coiba National Park, Republic of Panama, in February 2010 (07° 41'.723 N, 81° 38'.025 W). The samples were stored in 1:1 EtOH-H₂O and frozen at –20 °C prior to extraction. Morphological and molecular characterizations as well as phylogenetic analyses on *Lyngbya majuscula* (PNG 5-22-05-3) are described elsewhere.¹¹ Morphological characterization on *Oscillatoria* sp. was performed using an Olympus IX51 epifluorescent microscope (1000 \times) equipped with an Olympus U-CMAD3 camera. Morphological comparison and putative taxonomic identification of the cyanobacterial specimen was performed in accordance with modern classification systems.²⁰ These results were consistent with a phylogenetic analysis of this organism using the 16S rRNA subunit, as detailed elsewhere.²²

Extraction and Isolation

L. majuscula and *Oscillatoria* sp. were extracted separately with 2:1 CH₂Cl₂-MeOH and concentrated to dryness in vacuo to give 8.8 g and 91.0 mg of crude extract, respectively. Separated VLC prefractionation of the crude extracts using a gradient with 0–100% EtOAc in hexanes followed by 0–100% of MeOH in EtOAc yielded nine fractions (A–I). VLC fraction H from *L. majuscula* eluted with 25% MeOH in EtOAc (1.5 g), and was further fractionated by flash column chromatography on silica gel using a stepwise gradient of MeOH in CH₂Cl₂ to yield nine sub-fractions (H1 to H9). Fraction H2 was purified by reversed-phase HPLC (continuous gradient from 60:40 MeOH/H₂O to 100% MeOH in 65 min at 2 mL/min) to give 2.9 mg of serinolamide A (**3**) as a pale yellow oil (0.03%). VLC

fractions A (eluted with 100% hexanes, 1.3 mg) and B (eluted with 10% EtOAc in hexanes, 22.0 mg) from *Oscillatoria* sp. were combined according to their ^1H NMR, LCMS and TLC profiles, and subjected to ^1H NMR-guided fractionation using silica gel column chromatography (10% EtOAc in hexanes) to yield 6.6 mg (0.1%) of propenediester (**4**).

Serinolamide (3)—pale yellow, oil $[\alpha]_{\text{D}}^{25} + 2.6$ (*c* 0.28, CHCl_3); IR (film) λ_{max} 3351 (br), 2930, 2853, 1622, 1457, 1404, 1099, 1047 cm^{-1} ; ^1H and ^{13}C NMR, see Table 1; ESIMS m/z 384 (75) $[\text{M} + \text{H}]^+$, 767 (100) $[2 \text{M} + \text{H}]^+$; HRESITOFMS m/z $[\text{M} + \text{H}]^+$ 384.3479 (calcd for $\text{C}_{23}\text{H}_{46}\text{NO}_3$, 384.3472).

Propenediester (4)—colorless oil; IR (neat) 3005, 2926, 2855, 1746, 1371, 1224, 1136, 1029, 895 cm^{-1} ; ^1H , ^{13}C , and 2D NMR data, see Table 2; HRESITOFMS m/z $[\text{M} + \text{Na}]^+$ 417.2978 (calcd for $\text{C}_{24}\text{H}_{42}\text{O}_4\text{Na}$, 417.2975).

Derivatization of Serinolamide (3) with (*R*)- and (*S*)-9-AMA Acids

Esters **3a** and **3b** were prepared separately by treatment of serinolamide (**3**) (1 mg) with the corresponding (*R*)- and (*S*)-9-AMA acids (1.1 equivalents) in the presence of EDC (1.1 equivalents) and DMAP (catalytic) in dry CH_2Cl_2 , under a N_2 atmosphere. The reaction was stirred at room temperature for 12 h. The organic layer was washed sequentially with H_2O , HCl (1 M), H_2O , NaHCO_3 (sat) and H_2O , then dried (Na_2SO_4) and concentrated under reduced pressure to obtain the corresponding ester. Final purification was achieved by flash column chromatography on silica gel 230–400 mesh (elution with hexanes/ethyl acetate mixtures) to yield 2.2 mg of **3a** and 1.4 mg of compound **3b**.

(*R*)-9-AMA Ester Derivative (3a)— $[\alpha]_{\text{D}}^{25} - 10.1$ (*c* 1.4, CHCl_3); ^1H NMR (500 MHz, $\text{DMSO}-d_6$) δ 4.37 (1H, m, H-21), 4.08 (1H, dd, $J = 7.2, 11.4$ Hz, H-20a), 4.0 (1H, dd, $J = 5.3, 11.4$ Hz, H-20b), 3.08 (1H, m, H-22a), 2.98 (1H, dd, $J = 5.5, 10.1$ Hz, H-22b), 2.94 (3H, s, H-23), 2.16 (3H, s, H-19); HRESITOFMS m/z $[\text{M} + \text{H}]^+$ 632.4313 (calcd for $\text{C}_{40}\text{H}_{58}\text{NO}_5$, 632.4310).

(*S*)-9-AMA Ester Derivative (3b)— $[\alpha]_{\text{D}}^{25} + 10.1$ (*c* 0.93, CHCl_3); ^1H NMR (500 MHz, $\text{DMSO}-d_6$) δ 4.46 (1H, m, H-21), 4.07 (1H, dd, $J = 8.5, 11.6$ Hz, H-20a), 3.94 (1H, dd, $J = 4.55, 11.5$ Hz, H-20b), 2.89 (3H, s, H-23), 2.88 (1H, bs, H-22a), 2.87 (1H, bs, H-22b), 1.97 (3H, s, H-19); HRESITOFMS m/z $[\text{M} + \text{H}]^+$ 632.4304 (calcd for $\text{C}_{40}\text{H}_{58}\text{NO}_5$, 632.4310).

CB₁ and CB₂ Receptor Binding Assays

Membranes from HEK-293 cells, stably transfected with either the human recombinant CB₁ receptor ($B_{\text{max}} = 2.5$ pmol/mg protein) or human recombinant CB₂ receptor ($B_{\text{max}} = 4.7$ pmol/mg protein), were incubated with [^3H]CP-55,940 (0.14 nM/ $K_d = 0.18$ nM and 0.084 nM/ $K_d = 0.31$ nM, respectively, for CB₁ and CB₂ receptors) as the high affinity ligand. This ligand was then displaced with 10 μM WIN 55212-2 as the heterologous competitor for non specific binding (K_i values 9.2 nM and 2.1 nM, respectively, for CB₁ and CB₂ receptors). The two compounds were tested in a preliminary screening following the procedure described by the manufacturer (Perkin Elmer, Milano, Italy). The compound that displaced [^3H]CP-55,940 by more than 50% at 10 μM was further analyzed by carrying out a complete concentration-response curve (using 10, 100, 500, 1000, 2500, 10000 nM concentrations). Displacement curves were generated by incubating test compounds for 90 min at 30 °C with [^3H]CP-55,940 (0.14 nM and 0.084 μM in CB₁ and CB₂ binding assays, respectively). K_i values were calculated by applying the Cheng-Prusoff equation to the IC_{50} values (obtained by GraphPad) for the displacement of the bound radioligand by increasing concentrations of the test compounds. Data are means \pm SEM of $n = 3$ experiments.

Supplementary Material

Refer to Web version on PubMed Central for supplementary material.

Acknowledgments

We gratefully acknowledge the governments of Panamá and Papua New Guinea for permission to make the organism collections. M.G. thanks SENACYT, Panamá for financial support; H.M.D. thanks FAPESP, Brazil for providing a fellowship. Special thanks are due to Dr. R. Riguera for kindly providing the (*R*)- and (*S*)-9-AMA acids for stereochemical analysis. We also thank K. Tidgewell and C. Sorrels for help with the cyanobacterial collections, N. Engene for identification of the source cyanobacterium, Y. Su (UCSD) for the MS data acquisition, and F. Freire and J. Seco for comments on the stereochemical analysis. This work was supported by NIH CA 10085, CA 52955 and the Fogarty International Center' International Cooperative Biodiversity Groups program (grant number TW006634).

References

1. Felder CC, Glass M. *Annu. Rev. Pharmacol. Toxicol.* 1998; 38:179–200. [PubMed: 9597153]
2. Lambert DM, Fowler CJ. *J. Med. Chem.* 2005; 48:5059–5087. [PubMed: 16078824]
3. Stott CG, Guy GW. *Euphytica.* 2004; 140:83–93.
4. Howlett AC, Barth F, Bonner TI, Cabral G, Casellas P, Devane WA, Felder CC, Herkenham M, Mackie K, Martin BR, Mecholaum R, Pertwee RG. *Pharmacol. Rev.* 2002; 54:161–202. [PubMed: 12037135]
5. Marzo VD, Petrocellis LD. *Annu. Rev. Med.* 2006; 57:553–574. [PubMed: 16409166]
6. Pacher P, Batkai S, Kunos G. *Pharmacol. Rev.* 2006; 58:389–462. [PubMed: 16968947]
7. Devane WA, Hanus L, Breuer A, Pertwee RG, Stevenson LA, Griffin G, Gibson D, Mandelbaum A, Etinger A, Mechoulam R. *Science.* 1992; 258:1946–1949. [PubMed: 1470919]
8. Gonsiorek W, Lunn C, Fan X, Narula S, Lundell D, Hipkin W. *Mol. Pharmacol.* 2000; 57:1045–1050. [PubMed: 10779390]
9. Mecholaum R, Shabat SB, Hanus L, Ligumsky M, Kaminski NE, Schatz AR, Gopher A, Almong A, Martin BR, Compton DR, Pertwee RG, Griffin G. *Biochem. Pharmacol.* 1995; 50:83–90. [PubMed: 7605349]
10. (a) Soderstrom K, Murray TF, Yoo HD, Ketchum S, Milligan K, Gerwick W, Ortega MJ, Salva J. *Adv. Exp. Med. Biol.* 1997; 433:73–77. [PubMed: 9561107] (b) Pereira A, Pfeifer TA, Grigliatti TA, Andersen RJ. *ACS Chem. Biol.* 2009; 4:139–144. [PubMed: 19175306] (c) Bisogno T, Melck D, De Petrocellis L, Bobrov MY, Gretskey NM, Bezuglov VV, Sitachitta N, Gerwick WH, Di Marzo V. *Biochem. Biophys. Res. Commun.* 1998; 248:515–522. [PubMed: 9703957] (d) Han B, McPhail KL, Ligresti A, Di Marzo V, Gerwick WH. *J. Nat. Prod.* 2003; 66:1364–1368. [PubMed: 14575438]
11. Gutiérrez M, Suyama TL, Engene N, Wingerd JS, Matainaho T, Gerwick WH. *J. Nat. Prod.* 2008; 71:1099–1103. [PubMed: 18444683]
12. Gunstone FD, Pollard MR, Scrimgeour CM, Vedanayagam HS. *Chem. Phys. Lipids.* 1977; 18:115–129. [PubMed: 832335]
13. Freire F, Seco JM, Quiñoá E, Riguera R. *Chem. Commun.* 2007:1456–1458.
14. Tidgewell, K.; Clark, BT.; Gerwick, WH. *Comprehensive Natural Products Chemistry*. 2nd Ed. Moore, B.; Crews, P., editors. Oxford, UK: Pergamon Press; 2010. p. 141–188.
15. Malfitano AM, Ciaglia E, Gangemi G, Gazzerri P, Laezza C, Bifulco M. *Expert Opin. Ther. Targets.* 2011; 15:297–308. [PubMed: 21244344]
16. Milman G, Maor Y, Abu-Lafi S, Horowitz M, Gallily R, Batkai S, Mo FM, Offertaler L, Pacher P, Kunos G, Mechoulam R. *Proc. Natl. Acad. Sci. USA.* 2006; 103:2428–2433. [PubMed: 16467152]
17. Colman B, Norman E. *Physiol. Plant.* 1997; 100:133–136.
18. Jones AC, Monroe EA, Eisman EB, Gerwick L, Sherman D, Gerwick WH. *Nat. Prod. Rep.* 2010; 27:1048–1065. [PubMed: 20442916]
19. Geders TW, Gu L, Mowers JC, Liu H, Gerwick WH, Hakansson K, Sherman DH, Smith JL. *J. Biol. Chem.* 2007; 282:35954–35963. [PubMed: 17928301]

20. (a) Geitler, L. Cyanophyceae. Rabenhorst, L., editor. Leipzig: Akademische Verlag; 1932. p. 1060-1061. reprint: Koeltz Scientific Books: Königstein, 1985(b) Komárek, J.; Anagnostidis, K. Süwasserflora Von Mitteleuropa. Büdel, B.; Gartner, G.; Krienitz, L.; Schagerl, M., editors. Vol. 19/2. Jena: Gustav Fischer; 2005. p. 483-606.
21. Mevers E, Liu WT, Engene N, Mohimani H, Byrum T, Pevzner PA, Dorrestein PC, Spadafora C, Gerwick WH. *J. Nat. Prod.* 2011; 74:928–936. [PubMed: 21488639]
22. Malloy KL, Suyama TL, Engene N, Debonis H, Cao Z, Matainaho T, Di Marzo V, Spadafora C, Murray TF, Gerwick WH. *J. Nat. Prod.* (in review).

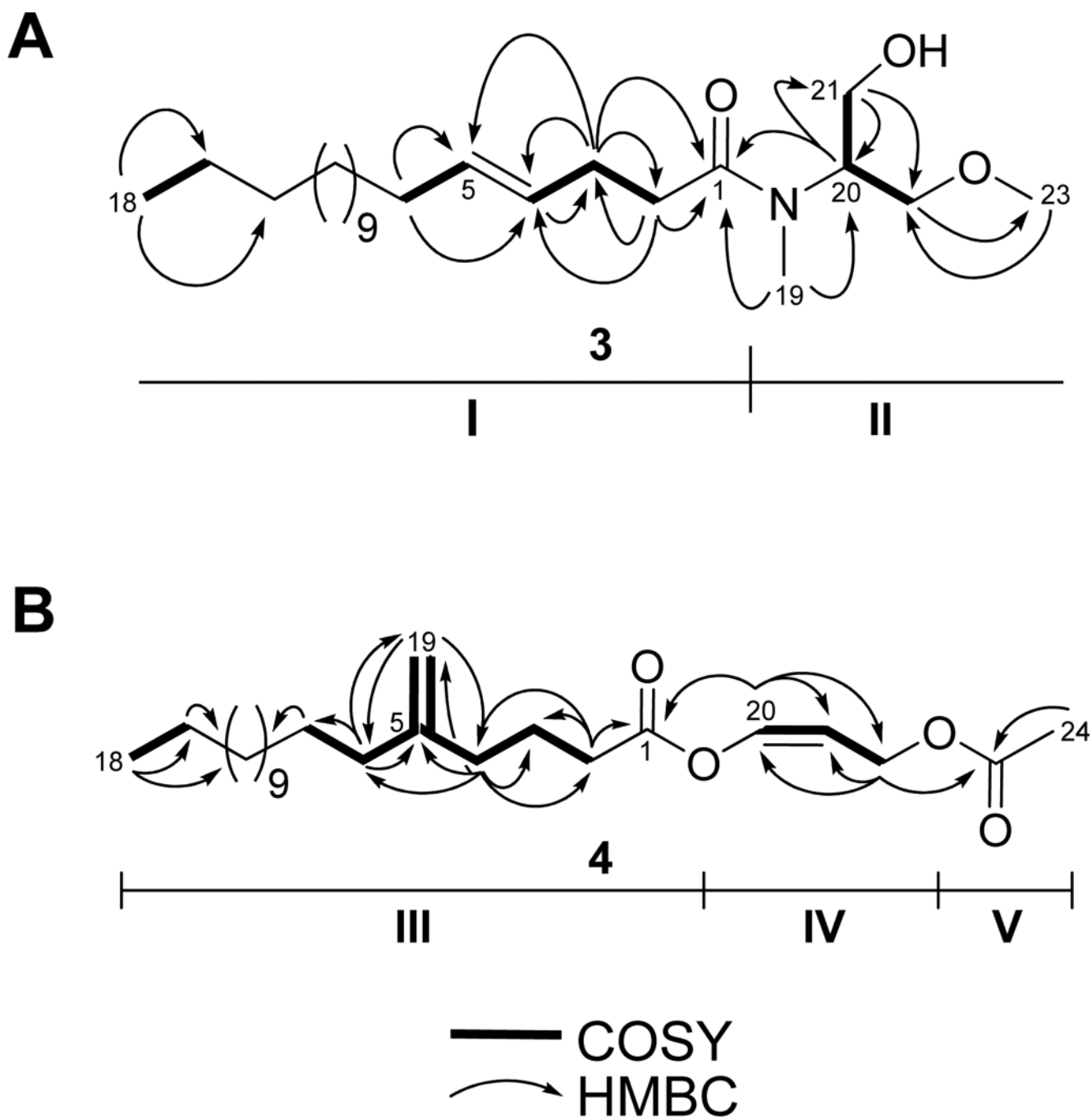


Figure 1.
Assembly of compounds **3** (A) and **4** (B) from their 2D-NMR data.

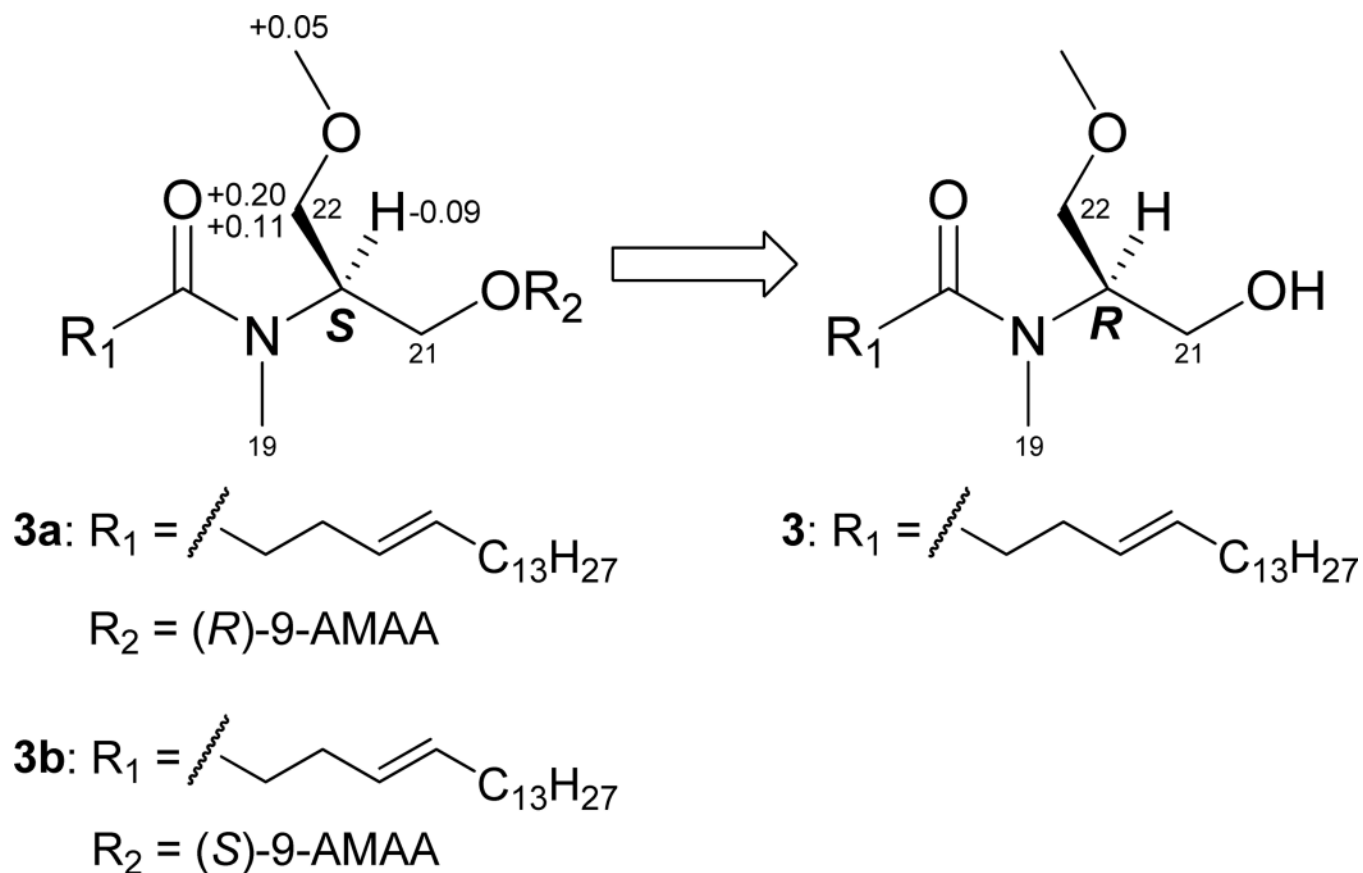
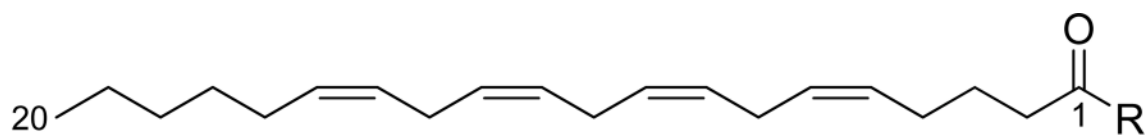


Figure 2. $\Delta\delta^{\text{RS}}$ values (ppm, DMSO- d_6) for the 9-AMA esters **3a** and **3b**. The priority order of the substituents at C-20 change when $R_2 = \text{H}$, thus the natural product **3** possesses an *R* configuration at C-20.



1 R = NHCH₂CH₂OH

2 R = OCH(CH₂OH)₂

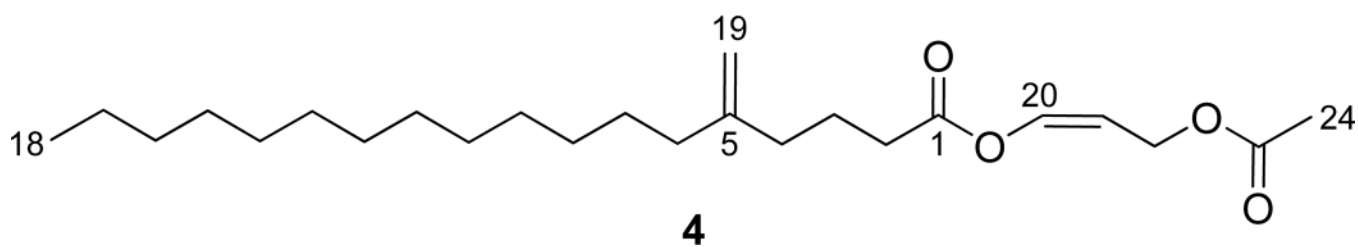
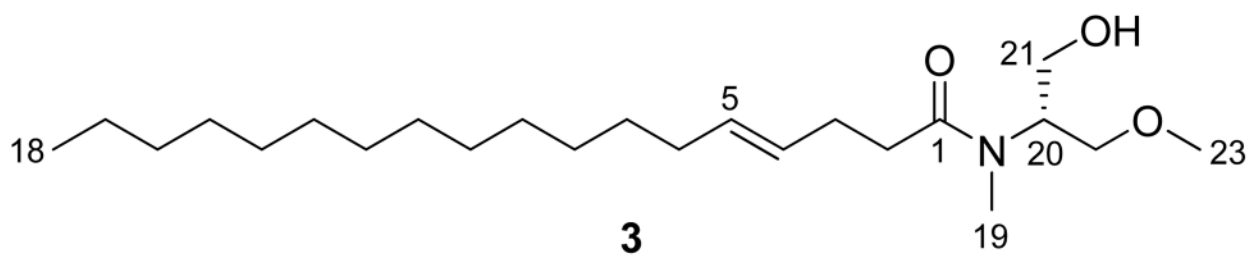


Table 1NMR Spectroscopic Data (500 MHz, CDCl₃) for Serinolamide A (**3**).

carbon	δ_C , mult. ^a	δ_H , mult. (J in Hz) ^b	HMBC ^c	COSY
1	174.3, C			
2	34.3, CH ₂	2.40, m	1, 3, 4	3
3	28.1, CH ₂	2.32, m	1, 2, 4, 5	2, 4
4	128.4, CH	5.43, m	3	3, 5
5	131.6, CH	5.47, m	6	4, 6
6	32.6, CH ₂	1.96, dd (6.5, 13.5)	4, 5, 7	5
7	29.5, CH ₂	1.25, m		
8 ^d	29.2, CH ₂	1.25, m		
9 ^d	29.3, CH ₂	1.25, m		
10 ^d	29.64, CH ₂	1.25, m		
11–15 ^d	29.68, 5 × CH ₂	1.25, m		
16	31.9, CH ₂	1.25, m		
17	22.7, CH ₂	1.28, m	14, 16	18
18	14.1, CH ₃	0.88, t (6.5)	16, 17	17
19	33.8, CH ₃	3.01, s	1, 20	
20	57.8, CHs	4.39, m	1, 19, 21, 22	21, 22
21	62.3, CH ₂	3.78, m	20, 22	20
22	71.0, CH ₂	3.66, dd (7.0, 10.0)	20, 21, 23	20
		3.56, dd (4.5, 10.0)	20, 21, 23	20
23	58.9, CH ₃	3.33, s		

^aRecorded at 125 MHz.^bRecorded at 500 MHz.^cFrom proton to the indicated carbon.^dAssignments may be interchanged.

Table 2NMR Spectroscopic Data (600 MHz, CDCl₃) for Propenediester (**4**).

Carbon	δ_C , mult. ^a	δ_H , mult. (J in Hz) ^b	HMBC ^c	COSY
1	170.1, C			
2	33.3, CH ₂	2.43, t (7.4)	1, 3, 4	3, 4
3	22.4, CH ₂	1.81, tt (7.4, 7.6)	1, 2, 5	2, 4
4	35.1, CH ₂	2.06, t (7.6)	2, 3, 5, 6, 19	2, 3, 6, 19
5	148.5, C			
6	35.8, CH ₂	1.99, t (7.6)	5, 7, 19	4, 7, 19
7	27.7, CH ₂	1.40, tt (6.8, 7.6)	8	6, 8
8	29.7, CH ₂	1.25, m		7
9–12 ^d	29.6, 4 × CH ₂	1.25, m		
13 ^d	29.5, CH ₂	1.25, m		
14 ^d	29.4, CH ₂	1.25, m		
15 ^d	29.3, CH ₂	1.25, m		
16	31.9, CH ₂	1.25, m		17
17	22.7, CH ₂	1.28, m	16	16, 18
18	14.1, CH ₃	0.88, t (7.1)	16, 17	17
19	109.7, CH ₂	4.73, d (16.6)	4, 6	4, 6
20	136.9, CH	7.23, dt (1.5, 6.5)	1, 21, 22	21, 22
21	107.4, CH	5.08, dt (6.5, 7.1)	20	20, 22
22	57.9, CH ₂	4.72, dd (1.5, 7.1)	20, 21, 23	20, 21
23	170.8, C			
24	20.9, CH ₃	2.07, s	23	

^aRecorded at 125 MHz.^bRecorded at 500 MHz.^cFrom proton to the indicated carbon.^dAssignments may be interchanged.

Table 3CB₁ and CB₂ Receptor Affinity of Compounds **3** and **4**.

Compound	CB ₁ IC ₅₀ (μM)	CB ₂ IC ₅₀ (μM)
Δ ⁹ -THC ^a	0.0028	0.0095
3	2.3 ± 0.1 ^b	>10
4	>10	>10

^aPositive control.^bK_i = 1.3 μM.